

Heat transfer in an insulated exhaust pipe

S. RJASANOW

Fachbereich Mathematik, Universität Kaiserslautern, 67653 Kaiserslautern, Germany

Received 31 January 1994; accepted in revised form 1 February 1994

Abstract. The warm-up cycle for an automobile engine with an insulated exhaust pipe between the engine and the catalytic converter is considered. The mathematical model for the heat transfer in the insulated exhaust pipe is presented. An efficient numerical algorithm for this model is also constructed and the numerical results are obtained and compared with measurements. Some possibilities for the geometrical optimization of the exhaust pipe are discussed.

1. Introduction

The use of catalytic converters has been an important method to reduce the CO, NO_x and various hydrocarbons in the exhaust of an automobile engine. Because of actual and future government regulations for emission control in industrial countries, there is a continuous urgency to improve the efficiency of catalytic converters and predict the output.

During the so-called warm-up cycle (2 or 3 minutes after every cold start), the temperature of the converter is too low for the catalytic reactions to take place and the converter, consequently operates inefficiently. There are different ideas to improve performance of the catalytic converter during the warm-up cycle. The practical experiments to verify these ideas are in general very expensive and also on the other hand very difficult because of the extreme nonstationary character of the warm-up cycle. Nowadays, the mathematical modelling and the numerical solution with the help of a computer is one of the most efficient tools to solve such complicated technical problems.

One of the first mathematical models for the catalytic converter was published in 1968 by Vardi and Biller [1] (one-dimensional model without considering any chemical reactions). Since then, more complicated mathematical models were discussed by many authors (see K. Zygourakis 1989 [2] and H.-J. Becker 1992 [3] for more references). In [9], a mathematical model is presented for the warm-up cycle with an additional warming device at the beginning of the catalytic converter. There is also a new concept of constructing an exhaust pipe between the engine and the catalytic converter (Nording, 1991, [10]). The most important features of this concept are

- insulated construction of an exhaust pipe with a double wall;
- air-tight outer wall with a carrying capacity;
- inner wall from light-gauge steel sheet.

The main idea of this concept is to prevent as much as possible the heat produced by the engine from getting lost on the way to the catalytic converter during the warm-up cycle. In this paper we deal with this concept mathematically for the case of rotational symmetry and also we realize it numerically.

The paper is organized as follows. In Section 2, we derive the mathematical model for the

heat transfer in an insulated exhaust pipe by consideration of conduction, convection and radiation of the heat and discuss the specific parameter settings.

In Section 3, we describe the standard numerical algorithm to solve the two-dimensional heat equation. Also we formulate here a new and very efficient algorithm for the numerical solution of the boundary integral equation for the radiation heat transfer.

In Section 4 the results of our numerical tests lead to some recommendations for geometrical optimization of such exhaust pipes and enable us to draw some conclusions.

2. Mathematical model

We consider a straight insulated exhaust pipe of the length $S[m]$ whose cross-section is shown in Fig. 1. The radii $R_1, R_2, R_3, R_4 [m]$ describe the thicknesses of the inner ($R_2 - R_1$) and outer ($R_4 - R_3$) walls. The thickness of the insulating air split is $R_3 - R_2$. We consider the following physical processes in the exhaust pipe:

1. Heat transfer due to forced convection in the inner pipe.
2. Heat transfer due to conduction within and between both walls of the exhaust pipe.
3. Heat transfer due to radiation in the insulating split.

We neglect the heat conduction in the exhaust gas flow in the inner pipe and the natural convection of the air in the insulating split.

We assume that the flow of the exhaust gas in the inner pipe is fully turbulent, there is no pressure gradient in the gas and the temperature of the exhaust gas is constant in each cross-section of the inner pipe.

We will use cylindrical coordinates (r, ϕ, z) with

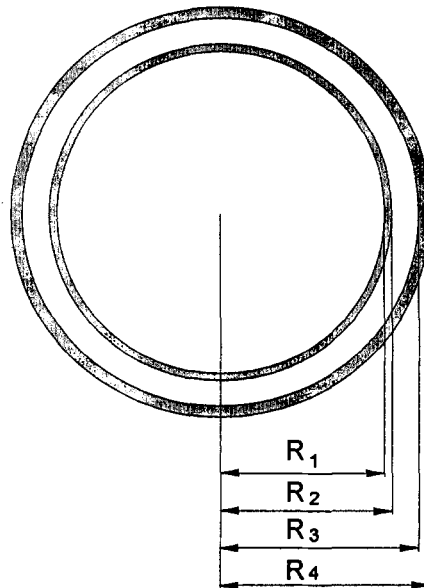


Fig. 1. The cross-section of the exhaust pipe.

$$0 \leq r \leq R_4, \quad 0 \leq \phi < 2\pi, \quad 0 \leq z \leq S,$$

because of the rotational symmetry of the problem.

With the help of the previous assumptions we formulate the following subsections:

1. The one-dimensional heat transfer equation for the temperature of the exhaust gas

$$T_{\text{gas}} = T_{\text{gas}}(t, z), \quad t \geq 0, \quad 0 \leq z \leq S.$$

2. The two-dimensional heat transfer equation for the temperature of the walls and of the air in the insulating split

$$T = T(t, r, z), \quad t \geq 0, \quad R_1 \leq r \leq R_4, \quad 0 \leq z \leq S.$$

3. The boundary integral equation for the reflected part of the radiation energy on the outer surface of the inner wall and on the inner surface of the outer wall

$$R = R(t, r, z), \quad t \geq 0, \quad r = R_2, R_3, \quad 0 \leq z \leq S.$$

The connection between the exhaust gas equation 1 and the heat transfer equation 2 will be formulated as a boundary condition for the heat transfer equation 2. The interface conditions

$$[T] \Big|_{r=R_2, R_3} = 0; \quad \left[k \frac{\partial T}{\partial n} \right] \Big|_{r=R_2, R_3} = Q(r, z)$$

($Q(r, z)$, $r = R_2, R_3$, $0 \leq z \leq S$ denotes the additional heat flux due to radiation) connect the heat transfer equation 2 with the radiation boundary integral equation 3. $[]$ denotes the jump of the function on the given surface. On the boundary $r = R_4$ we formulate the boundary condition for the heat equation 2 due to natural convection and radiation.

2.1. Exhaust gas flow

The input parameters for the exhaust gas flow are

$T_{\text{gas}}(t, 0)$ [K] the temperature of the exhaust gas at the inlet of the exhaust pipe;

$m_{\text{gas}}(t)$ [kg/h] input rate of the exhaust gas;

p_{gas} [bar] pressure of the exhaust gas.

The velocity of the exhaust gas at the inlet of the exhaust pipe can be computed by the given temperature and pressure from the input rate and from the state equation

$$p_{\text{gas}} = \rho \bar{R} T_{\text{gas}} \quad (\bar{R}\text{-specific gas konstant for air):}$$

$$v_{\text{gas}}(t) = \frac{m_{\text{gas}} \bar{R} T_{\text{gas}}}{3600 \pi R_1^2 p_{\text{gas}}} [m/s].$$

Now we are able to model the heat transfer equation for the exhaust gas in the exhaust pipe $T_{\text{gas}}(t, z)$, $t \geq 0$, $0 \leq z \leq S$ using the boundary data $T_{\text{gas}}(t, 0)$ and $v_{\text{gas}}(t)$, $t \geq 0$. The heat flux through the boundary of the pipe per square meter per second is given by the formula

$$-H(t)(T_{\text{gas}}(t, z) - T(t, R_1, z)) \quad (1)$$

where $T(t, R_1, z)$ is the temperature of the inner wall of the inner pipe. Now we derive the heat transport equation for $T_{\text{gas}}(t, z)$. For this purpose we consider the cylinder

$$\{(r, w) : 0 \leq r \leq R_1, \quad z \leq w \leq z + \alpha\}$$

of the small thickness $\alpha \ll 1$ and assume that the temperature of the gas within this cylinder is constant and equal to $T_{\text{gas}}(t, z)$. After a small interval of time Δt this cylinder is at the position $z + \Delta z$ with the temperature $T_{\text{gas}}(t + \Delta t, z + \Delta z)$. The loss of the energy

$$(T_{\text{gas}}(t, z) - T_{\text{gas}}(t + \Delta t, z + \Delta z))\pi R_1^2 \alpha \rho c$$

(ρ denotes the density and c the specific heat for the exhaust gas) must be equal to the energy transfer through the boundary of our cylinder from exhaust gas to the steel wall of the pipe within the time $\Delta t = \Delta z / v_{\text{gas}}(t)$

$$(T_{\text{gas}}(t, z) - T_{\text{gas}}(t + \Delta t, z + \Delta z))\pi R_1^2 \alpha \rho c = H(t)(T_{\text{gas}}(t, z) - T(t, R_1, z))2\pi R_1 \alpha \Delta t .$$

For $\Delta t \rightarrow 0$ we obtain the first equation of our system:

$$\rho c \left(\frac{\partial T_{\text{gas}}(t, z)}{\partial t} + v(t) \frac{\partial T_{\text{gas}}(t, z)}{\partial z} \right) = -\frac{2}{R_1} H(t)(T_{\text{gas}}(t, z) - T(t, R_1, z)), \quad 0 < z \leq S \quad (2)$$

with the initial condition

$$T_{\text{gas}}(0, z) = T_0$$

and the boundary condition

$$T_{\text{gas}}(t, z)|_{z=0} = T_{\text{gas}}(t, 0) .$$

Equation (2) is a non-linear partial differential equation of the first order.

2.2. Conduction heat transfer

The conduction heat transfer takes place between inner wall of the inner pipe and outer wall of the outer pipe. This domain is shown in cylindrical coordinates in Fig. 2. The heat transfer equation for $T = T(t, r, z)$ has the following form:

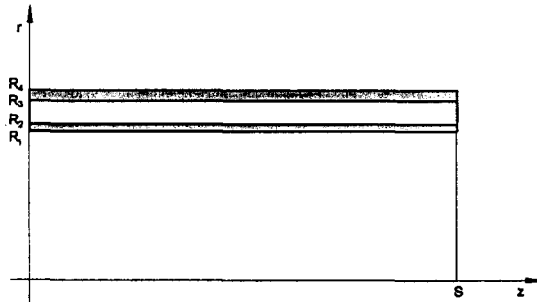


Fig. 2. The domain for the heat transfer equation (3).

$$\rho c \frac{\partial T}{\partial t} = \frac{1}{r} \frac{\partial}{\partial r} \left(r k \frac{\partial T}{\partial r} \right) + \frac{\partial}{\partial z} \left(k \frac{\partial T}{\partial z} \right), \quad R_1 < r < R_4, \quad 0 < z < S, \quad (3)$$

with the boundary conditions

$$\begin{aligned} -k \frac{\partial T}{\partial r} &= H(T_{\text{gas}} - T) && \text{for } r = R_1 \text{ (see (1))}; \\ k \frac{\partial T}{\partial r} &= H(T_0 - T) + \varepsilon_0 \sigma (T_0^4 - T^4) && \text{for } r = R_4 \text{ (see Subsection 2.4)}; \\ -k \frac{\partial T}{\partial z} &= 0 && \text{for } z = 0; \\ k \frac{\partial T}{\partial z} &= 0 && \text{for } z = S; \end{aligned}$$

and the interface conditions

$$\begin{aligned} [T] &= 0 && \text{for } r = R_2, R_3; \\ \left[k \frac{\partial T}{\partial r} \right] &= Q(r, z) && \text{for } r = R_2, R_3. \end{aligned}$$

2.3. Radiation

The heat transfer due to radiation takes place in the insulating split and from the outer surface of the pipe to the neighborhood. This last radiation heat transfer we take into consideration with the help of the boundary condition on the surface $r = R_4$:

$$\varepsilon_0 \sigma (T_0^4 - T^4). \quad (4)$$

The thermal radiation analysis in the insulating pipe is more complicated and we will derive a boundary integral equation for the reflected part of radiation energy. We fix first two points x and y on the boundary

$$\Gamma = \Gamma_1 \cup \Gamma_2,$$

where Γ_1 is the outer surface of the inner pipe and Γ_2 is the inner surface of the outer pipe. We neglect the influence of both the circular covers

$$\{(r, z) : R_2 \leq r \leq R_3, \quad z = 0, S\}.$$

If we assume that we are dealing with a 'black body', then the heat transmitted from differential element ds_x to differential element ds_y is

$$dE_{x \rightarrow y} = \frac{1}{\pi} \sigma T^4(x) \frac{(n_x, y-x)(n_y, x-y)}{|x-y|^4} ds_x ds_y$$

(see f.e. [4]). The total energy leaving all of the surface Γ that reaches the element ds_y is then

$$E_{\Gamma \rightarrow y} = \frac{1}{\pi} \int_{\Gamma} \kappa(x, y) \sigma T^4(x) \frac{(n_x, y-x)(n_y, x-y)}{|x-y|^4} ds_x ds_y,$$

where $\kappa(x, y)$ denotes the visibility function:

$$\kappa(x, y) = \begin{cases} 1 & x \text{ is visible from } y, \\ 0 & x \text{ is not visible from } y. \end{cases}$$

The heat flux due to radiation in point y is given by

$$Q(y) = (\mathcal{B}u)(y) - u(y)$$

where

$$u(y) = \sigma T^4(y),$$

$$(\mathcal{B}u)(y) = \frac{1}{\pi} \int_{\Gamma} \kappa(x, y) u(x) \frac{(n_x, y-x)(n_y, x-y)}{|x-y|^4} ds_x.$$

It means that if we have the temperature $T(x)$ everywhere on the boundary Γ , then we are able to compute the radiation heat flux on the boundary through the evaluation of the boundary integral operator \mathcal{B} at the point y .

A body that is not black will absorb and emit less than the black body radiation:

$$u(y) = \varepsilon \sigma T^4(y), \quad 0 < \varepsilon < 1. \quad (5)$$

If we denote the reflected part of the energy reaching the point $y \in \Gamma$ by $R(y)$ then the heat flux at y is

$$Q(y) = \varepsilon((\mathcal{B}u(x))(y) + R(y)) - u(y). \quad (6)$$

In order to derive the equation for $R(y)$ we assume that diffuse reflection takes place or that the reflected part of the energy

$$R_-(y) = (1 - \varepsilon)((\mathcal{B}u(x))(y) + R(y))$$

will be distributed on the same way as the radiated part:

$$R(y) = (\mathcal{B}R_-(x))(y),$$

$$\text{or } R(y) = (1 - \varepsilon)(\mathcal{B}^2 u(x))(y) + (1 - \varepsilon)(\mathcal{B}R_-(x))(y),$$

$$\text{or } ((\mathcal{I} - (1 - \varepsilon)\mathcal{B})R(x))(y) = (1 - \varepsilon)(\mathcal{B}^2 u(x))(y). \quad (7)$$

This is a boundary integral equation (see also [5,6]) with respect to $R(x)$ of the second kind with a symmetric kernel

$$\frac{1}{\pi} \kappa(x, y) \frac{(n_x, y-x)(n_y, x-y)}{|x-y|^4} = K(x, y).$$

For the given temperature we solve equation (7) and compute the function $Q(y) = Q(r, z)$ with the help of (6) to get the interface condition for the heat equation (3).

2.4. Specific parameter setting

In order to use the mathematical model derived in the previous subsections for the practical computations, we have to discuss the choice of all specific parameters used in the model. We have three different materials: exhaust gas, steel and air in the insulating split.

Exhaust gas

For the exhaust gas flow in the inner pipe we need the following physical parameters: the heat transfer coefficient $H(t)$ and the product ρc . The correct physical parameters for the exhaust gas can be obtained from the corresponding parameters for the components of the exhaust gas with the help of tables of data (see f.e. [3,13]). As agreed with the Firm H. Gillet GmbH we have used the values for air.

The heat transfer coefficient $H[J/(m^2sK)]$ is defined by (see f.e. [4])

$$H = \frac{Nu k}{2R_1} \quad (8)$$

where Nu denotes the Nusselt number, $k[J/(msK)]$ the thermal conductivity and $2R_1$ is the diameter of the inner pipe. We use one of the empirical formulae for the thermal conductivity k (see [11])

$$k = \frac{9.71}{T_{\text{gas}} + 416.0} \left(\frac{T_{\text{gas}} + 291.0}{273.0} \right)^{3/2} \cdot \quad (9)$$

and the Dittus–Boelter equation for the Nusselt number

$$Nu = 0.023 Re^{0.8} Pr^{0.4}$$

where

$$Re = Re(t) = \frac{2R_1 v_{\text{gas}}(t)}{\nu(t)}$$

is the Reynolds number and

$$Pr = 0.689$$

denotes the Prandtl number. The exponent on the Prandtl number is chosen, since the process now is heating. We neglect the entrance effects by the definition of the Nusselt number.

The viscosity of the gas $\nu(t)$ varies with the average temperature $\bar{T}_{\text{gas}}(t)$ and can be obtained from the following table and from linear interpolation in-between.

The product ρc can be given by the formula

Table 1. Viscosity of the air for various values of temperature

$\nu \cdot 10^6 [m^2/s]$	15.68	25.9	37.9	51.3	66.2	82.3	99.3	117.8	138.6	159.1
$T_{\text{gas}} [K]$	300	400	500	600	700	800	900	1000	1100	1200

$$\rho c = \frac{1.07 \times 10^3 P_{\text{gas}}}{RT_{\text{gas}}(t)} \quad [\text{J}/(\text{m}^3\text{k})]. \quad (10)$$

Steel

We use the constants

$$\rho c = 35958.0 \quad [\text{J}/(\text{m}^3\text{K})]$$

for the product of the density and specific heat of the steel V2A and

$$k = 17.0 \quad [\text{J}/(\text{msK})]$$

for its thermal conductivity. The emissivity ε_0 of the outer wall of the outer pipe is assumed to be independent of wavelength (our pipe is so-called gray body). We have used the value

$$\varepsilon_0 = 0.9$$

and σ denotes in (4) the Boltzmann constant

$$\sigma = 5.669 \times 10^{-8} \quad [\text{J}/(\text{m}^2\text{sK}^4)].$$

The heat transfer coefficient H can be modeled for $r = R_4$ due to natural convection as follows:

$$H = \frac{Nu \, k}{\alpha},$$

where Nu is the Nusselt number

$$Nu = 0.59(Gr \, Pr)^{0.25},$$

k is the thermal conductivity of the air and α is the characteristic length:

$$\alpha = \begin{cases} S & \text{for the vertical position,} \\ 2R_4 & \text{for the horizontal position.} \end{cases}$$

The Grashof number Gr is given by

$$Gr = \frac{g\alpha^3}{\nu^2 T_0} (T - T_0),$$

where $g[\text{m}/\text{s}^2]$ denotes the acceleration due to gravity and ν is the kinematic viscosity. The Prandtl number Pr is again equal to 0.689.

The emissivity ε in equations (7) will be found in Subsection 4.1 by comparison of the numerical tests with the results of the measurements.

3. Numerical algorithm

The numerical method for the systems (2), (3), (7) is organized as follows:

1. We choose the time step $\tau > 0$ and both the space meshes h_1 in z -direction and h_2 in r -direction, where

$$h_1 = S/N_1 \quad \text{and} \quad h_2 = (R_4 - R_1)/N_2.$$

2. We compute $H(t)$ and ρc for the exhaust gas with the help of (8), (9) and Table 1 for the given temperature $T_{\text{gas}}(t, z)$ and $T(t, r, z)$ at the time point $t = m\tau, m = 0, \dots$
3. We solve equation (2) as in Subsection 3.1 to get the temperature $T_{\text{gas}}(t + \tau, z)$ and define the boundary condition for equation (3) on the boundary $r = R_1$.
4. We compute the right-hand side of the boundary integral equation (7) with the help of the given temperature $T(t, r, z), r = R_2, R_3$.
5. We solve the boundary integral equations (7) (Subsection 3.2) and compute the function $Q(r, z), r = R_2, R_3$ with the help of (6). After that we use this function in the interface condition for equation (3) on the boundaries $r = R_2, R_3$.
6. We compute $H(t)$ on the boundary $r = R_4$ and rewrite the boundary condition for equation (3) on this boundary in the form

$$k \frac{\partial T}{\partial r} = \tilde{H}(T_0 - T),$$

$$\tilde{H} = H(t) + \varepsilon_0 \sigma \frac{T_0^4 - T^4}{T_0 - T} = H(t) + \varepsilon_0 \sigma (T_0^3 + T_0^2 T + T_0 T^2 + T^3).$$

This boundary condition is now linearized.

7. Now we compute the heat conduction coefficient for the air in the insulating split and solve equation (3) to get $T(t + \tau, r, z)$ (Subsection 3.3).
8. When $m \leq m_{\text{max}}$, we repeat the algorithm beginning from step 2.

3.1. Numerical solution of the exhaust flow equation

We will use the usual differential scheme [14] for equation (2):

$$\begin{aligned} & \rho c \left(\frac{T_{\text{gas}}(t + \tau, z_k) - T_{\text{gas}}(t, z_k)}{\tau} + v_{\text{gas}} \frac{T_{\text{gas}}(t + \tau, z_k) - T_{\text{gas}}(t + \tau, z_{k-1})}{h_1} \right) \\ &= -\frac{2}{R_1} H(t) (T_{\text{gas}}(t + \tau, z_k) - T(t, R_1, z_k)), \end{aligned}$$

or

$$\begin{aligned} T_{\text{gas}}(t + \tau, z_k) &= \frac{a_1}{a_1 + a_2 + a_3} T_{\text{gas}}(t, z_k) + \frac{a_2}{a_1 + a_2 + a_3} T_{\text{gas}}(t + \tau, z_{k-1}) \\ &\quad + \frac{a_3}{a_1 + a_2 + a_3} T(t, R_1, z_k) \end{aligned}$$

$$a_1 = \frac{\rho c}{\tau}, \quad a_2 = \frac{\rho c v_{\text{gas}}}{h_1}, \quad a_3 = \frac{2}{R_1} H(t), \quad k = 2, \dots, N_1 + 1;$$

$$T_{\text{gas}}(t + \tau, z_1) = T_{\text{gas}}(t + \tau, 0),$$

$$T_{\text{gas}}(0, z_k) = T_0, \quad k = 1, \dots, N_1 + 1.$$

This differential scheme approximates equation (2) with first-order accuracy and it is stable. The number of arithmetical operations is of the capital order $O(N_1)$ per time step. We remark that $T_{\text{gas}}(t + \tau, S)$ is one of our most important output values.

3.2. Numerical solution of the boundary integral equation

We will use the piecewise constant functions

$$\varphi_i^{(\alpha)}(z) = \begin{cases} 1 & (r, \varphi, z) \in \Gamma_\alpha^{(i)} \\ 0 & \text{otherwise,} \end{cases} \quad i = 1, \dots, N_1, \quad \alpha = 1, 2$$

with

$$\Gamma_\alpha^{(i)} = \{(r, \varphi, z) : r = R_{\alpha+1}, z_i \leq z \leq z_{i+1}, 0 \leq \varphi < 2\pi\}$$

for the approximation of the solution of the boundary integral equation (7):

$$R(r, z) \approx \sum_{i=1}^{N_1} y_i^{(1)} \varphi_i^{(1)}(z) + \sum_{i=1}^{N_1} y_i^{(2)} \varphi_i^{(2)}(z) = \Phi_1 y_1 + \Phi_2 y_2,$$

$$\Phi_\alpha = (\varphi_1^{(\alpha)}, \dots, \varphi_{N_1}^{(\alpha)}), \quad y_\alpha \in \mathbb{R}^{N_1}, \quad \alpha = 1, 2.$$

The same form can be used for the approximation of the function u on the right-hand side of equation (7)

$$u(t, z) \approx \Phi_1 u_1 + \Phi_2 u_2$$

where the components of the vectors u_1 and u_2 can be computed as

$$u_i^{(\alpha)} = \sigma(0.5(T(t, R_{\alpha+1}, z_i) + T(t, R_{\alpha+1}, z_{i+1})))^4, \quad i = 1, \dots, N_1, \quad \alpha = 1, 2. \quad (11)$$

The Galerkin procedure for equation (7) leads to:

Find $y_1, y_2 \in \mathbb{R}^{N_1}$ such that Galerkin equations

$$\langle (\mathcal{J} - (1 - \varepsilon)\mathcal{B})(\Phi_1 y_1 + \Phi_2 y_2), \varphi_i^{(\alpha)} \rangle = (1 - \varepsilon) \langle \mathcal{B}^2(\Phi_1 u_1 + \Phi_2 u_2), \varphi_i^{(\alpha)} \rangle$$

are fulfilled for all $i = 1, \dots, N_1, \alpha = 1, 2$, where \langle, \rangle denotes the L_2 -scalar product:

$$\langle u, v \rangle = \int_{\Gamma} v u \, ds_x.$$

The Galerkin system of equations can be now rewritten in the form

$$Ay = b, \quad A \in \mathbb{R}^{2N_1 \times 2N_1}, y, b \in \mathbb{R}^{2N_1} \quad (12)$$

$$A = \begin{pmatrix} A_{11} & A_{12} \\ A_{21} & A_{22} \end{pmatrix}, \quad y = (y_1^T, y_2^T)^T, \quad b = (b_1^T, b_2^T)^T,$$

$$(A_{kl})_{ij} = \langle \varphi_j^{(l)}, \varphi_i^{(k)} \rangle = (1 - \varepsilon) \int_{\Gamma_k^{(l)}} \int_{\Gamma_l^{(j)}} K(x, y) \, ds_x \, ds_y, \quad k, l = 1, 2, i, j = 1, \dots, N_1,$$

$$(b_k)_i = (1 - \varepsilon) \int_{\Gamma_k^{(i)}} (\mathcal{B}^2(\Phi_1 u_1 + \Phi_2 u_2))(x) \, ds_x.$$

The matrix of the system (12) can also be computed as

$$A = 2\pi h_1 \begin{pmatrix} R_2^2 I & \mathcal{O} \\ \mathcal{O} & R_3^2 I \end{pmatrix} - (1 - \varepsilon) \begin{pmatrix} B_{11} & B_{12} \\ B_{21} & B_{22} \end{pmatrix},$$

and we will use the Matrix $B = \begin{pmatrix} B_{11} & B_{12} \\ B_{21} & B_{22} \end{pmatrix}$ for the approximation of the right-hand side b :

$$b \approx (1 - \varepsilon) B^2 u. \quad (13)$$

We are now dealing with the computation of the elements of the matrices B_{kl} , $k, l = 1, 2$. The matrix B_{11} is equal to zero, because of the visibility function

$$\kappa(x, y) = 0, \quad x, y \in \Gamma_1,$$

i.e. a convex body cannot radiate on itself.

The matrices B_{12} and B_{21} fulfill $B_{12} = B_{21}^T$ and the matrix B_{22} is symmetric i.e. $B_{22} = B_{22}^T$ because of the symmetry of the kernel of the operator \mathcal{B} . But the most important property of the matrices B_{12} and B_{22} is that they have Toeplitz structure. We consider first the elements of the matrix B_{12} (see Fig. 3):

$$(B_{12})_{ij} = \frac{1}{\pi} \int_{\Gamma_1^{(i)}} \int_{\Gamma_2^{(j)}} \kappa(x, y) \frac{(n_x, y - x)(n_y, x - y)}{|x - y|^4} \, ds_x \, ds_y,$$

or for

$$\begin{aligned} x &= R_2(\cos \varphi, \sin \varphi, z_x)^T, & y &= R_3(\cos \psi, \sin \psi, z_y)^T, \\ n_x &= (\cos \varphi, \sin \varphi, 0)^T, \end{aligned}$$

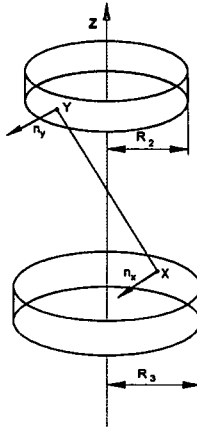


Fig. 3. On the computation of the Matrix B_{12} .

$$\begin{aligned}
n_y &= -(\cos \psi, \sin \psi, 0)^T, \\
(n_x, y-x) &= R_3 \cos(\varphi - \psi) - R_2, (n_y, x-y) = R_3 - R_2 \cos(\varphi - \psi), \\
|x-y|^2 &= R_2^2 + R_3^2 + (z_x - z_y)^2 - 2R_2R_3 \cos(\varphi - \psi), \\
\kappa(x, y) &= \begin{cases} 1, & \psi - \arccos(R_2/R_3) \leq \varphi \leq \psi + \arccos(R_2/R_3) \\ 0, & \text{elsewhere,} \end{cases} \\
ds_x &= R_2 d\varphi dz_x, ds_y = R_3 d\psi dz_y, \\
(B_{12})_{ij} &= \frac{R_2R_3}{\pi} \int_{z_i}^{z_i+h_1} dz_x \int_{z_j}^{z_j+h_1} dz_y \int_0^{2\pi} d\psi \int_{\psi-\arccos(R_2/R_3)}^{\psi+\arccos(R_2/R_3)} f(z_x, z_y, \psi, \varphi) d\varphi
\end{aligned}$$

with

$$f(z_x, z_y, \psi, \varphi) = \frac{(R_3 \cos(\varphi - \psi) - R_2)(R_3 - R_2 \cos(\varphi - \psi))}{(R_2^2 + R_3^2 + (z_x - z_y)^2 - 2R_2R_3 \cos(\varphi - \psi))^2}.$$

It is now easy to see the Toeplitz structure of B_{12} ($j \geq i$)

$$(B_{12})_{ij} = (B_{12})_{1, j-i+1} = 4R_2R_3 \int_0^{h_1} \int_0^{h_1} s(a, b, c, d, e, \varphi) dz_x dz_y, \quad (14)$$

where

$$\begin{aligned}
s(a, b, c, d, e, \varphi) &= \int_0^\varphi \frac{a \cos^2 \beta + b \cos \beta + c}{(d + e \cos \beta)^2} d\beta \\
&= \frac{a}{e^2} \varphi + \frac{b - \frac{2ad}{e}}{e} \frac{2}{\sqrt{d^2 - e^2}} \arctan \frac{\sqrt{d^2 + e^2} \operatorname{tg} \frac{\varphi}{2}}{d + e} \\
&\quad + \left(c - \frac{ad^2}{e^2} \right) \left(\frac{-e \sin \varphi}{(d^2 - e^2)(d + e \cos \varphi)} + \frac{2}{(d^2 - e^2)^{3/2}} \arctan \frac{\sqrt{d^2 + e^2} \operatorname{tg} \frac{\varphi}{2}}{d + e} \right),
\end{aligned}$$

$$a = -R_2 + R_3, b = R_2^2 + R_3^2, c = -R_2R_3,$$

$$d = R_2^2 + R_3^2 + (z_x - z_y + (i-j)h_1)^2, e = -2R_2R_3, \varphi = \arccos(R_2/R_3).$$

The matrix B_{22} has also the Toeplitz structure and can be computed as ($j \geq i$)

$$(B_{22})_{ij} = (B_{22})_{1, j-i+1} = 4R_3^4 \int_0^{h_1} \int_0^{h_1} s(a, b, c, d, e) dz_x dz_y, \quad (15)$$

$$a = 1, b = -2, c = 1,$$

$$d = 2R_3^2 + (z_x - z_y + (i-j)h_1)^2, e = -2R_3^2, \varphi = 2 \arccos(R_2/R_3).$$

It is necessary to compute only the elements $(B_{12})_{1j}, (B_{22})_{1j}$ for $j = 1, \dots, N_1$ with the help of the numerical integration in (14) and (15). We have used the trapezoidal rule for this

purpose. The numerical work for the computation of the matrix A is now reduced to $O(N_1)$ and must be done only once before the time steps begin as an initial step.

The next problem is to compute the right-hand side of equations (12) and to solve it. The matrix A of this equation is symmetric and positive definite (this is easy to see at least for $\varepsilon \approx 1$). Therefore, we can use Cholesky decomposition leading to $O(N_1^3)$ arithmetical operations or Conjugate Gradient Method (CGM) (see [7]). The convergence of the CGM depends on the spectral condition number of the Matrix $C^{-1}A$, where C denotes the so-called preconditioning matrix. Our system matrix A is the result of the Galerkin procedure for the integral operator of the second kind and its condition number is expected to be bounded by $N_1 \rightarrow \infty$:

$$\text{cond}_2(A) = O(1), \quad N_1 \rightarrow \infty.$$

We can therefore use the CGM without preconditioning ($C = I$) for iterative solution of (12) and the number of iterations required will be bounded by a constant with respect to N_1 . The CGM algorithm has the form:

1. $y_0 \in \mathbb{R}^n$;
 $r_0 = Ay_0 - b$;
 $w_0 = C^{-1}r_0$;
 $s_0 = w_0$;
2. for $k = 0, 1, \dots$ (16)

$$y_{k+1} = y_k - \alpha_{k+1}s_k, \quad \alpha_{k+1} = \frac{(r_k, w_k)}{(As_k, s_k)},$$

$$r_{k+1} = r_k - \alpha_{k+1}As_k ;$$

$$w_{k+1} = C^{-1}r_{k+1} ;$$

$$s_{k+1} = w_{k+1} + \beta_{k+1}s_k, \quad \beta_{k+1} = \frac{(r_{k+1}, w_{k+1})}{(r_k, w_k)},$$

where $n = 2N_1$ and $C = I$ for the system (12). The most expensive step of the algorithm (16) is now to compute the product As_k in each iteration. We will use the special structure of the matrix A (block Toeplitz structure) to construct an efficient algorithm for this purpose. The multiplication As_k can be obtained by four multiplications of a Toeplitz matrices with vectors of the length N_1 . The multiplication with the Toeplitz matrix Q of the dimension N_1 with a vector can be realized as follows. We define the matrix \tilde{Q} of the dimension $M = 2^m$ with $2N_1 \leq M \leq 4N_1$ and of the circulant structure in such a way that Q is placed as a \tilde{Q}_{11} block:

$$\tilde{Q} = \begin{pmatrix} Q & \tilde{Q}_{12} \\ \tilde{Q}_{21} & \tilde{Q}_{22} \end{pmatrix}.$$

It is well known [12] that the multiplication of the circulant matrix with a vector can be realized with only $O(M \ln M) = O(N_1 \ln N_1)$ arithmetical operations using Fast Fourier Transform (FFT). If we multiply the matrix \tilde{Q} with the vector $(s^T, 0)^T$ we will get $((Qs)^T, u^T)$ where Qs is what we need and u is not useful for us. Since all other steps in (16) need only $O(N_1)$ arithmetical operations and the number of iterations required to reach the

accuracy ε_s is $O(\ln \varepsilon_s^{-1})$, we get the total number of operations to solve the system (12) is of the capital order $O(N_1 \ln N_1 \ln \varepsilon_s^{-1})$ which is nearly optimal for this problem.

3.3. Numerical solution of the heat equation

The numerical procedure for equation (3) is standard: We use a five-point differential scheme for this equation and approximate the boundary conditions in such a way that second-order approximation is guaranteed also on the boundary. We compute necessary parameters like heat conduction coefficient, heat transfer coefficients, additional heat flux due to radiation on the boundaries $r = R_2, R_3$ and linearize the boundary condition on $r = R_4$ with the help of the given temperature $T(t, r, z)$ at the previous time step. The implicit differential scheme with respect to time leads in this case to a system of linear equations of the dimension

$$N = (N_1 + 1)(N_2 + 1).$$

We use the CGM (16) for the iterative solution of this system in each time step using the preconditioning technique which is known in literature as MIC* (0) [8] or MAF, leading to a number of arithmetical operations of $O(N^{5/4} \ln \varepsilon_h^{-1})$, where ε_h denotes the corresponding accuracy. Therefore this step is most expensive in the whole procedure.

4. Numerical tests

The numerical experiments were of two different kinds:

1. To verify the mathematical model and the numerical procedure with the help of measurements provided by the Firm 'H. Gillet GmbH', Edenkoben.
2. To give some recommendations for geometrical optimization of the exhaust pipe with the help of the numerical results.

4.1. Verification of the model

The following 'real' geometry was used for the measurements and for our tests:

$$R_1 = 0.0215 \text{ m}, \quad R_2 = 0.0225 \text{ m}, \quad R_3 = 0.026 \text{ m}, \quad R_4 = 0.0275 \text{ m}, \quad S = 1 \text{ m}.$$

The tests were done for the following two stationary situations:

$$\text{Test 1: } T_{\text{gas}}(t, 0) = 380^\circ\text{C}, \quad m_{\text{gas}}(t) = 24.5 \text{ kg/h}, \quad p_{\text{gas}} = 1.05 \text{ bar},$$

$$\text{Test 2: } T_{\text{gas}}(t, 0) = 690^\circ\text{C}, \quad m_{\text{gas}}(t) = 85 \text{ kg/h}, \quad p_{\text{gas}} = 1.05 \text{ bar}.$$

We have used six measurement points P_1, \dots, P_6 with

Table 2. Measurements for the test 1

Test 1	P_1	P_2	P_3	P_4	P_5	P_6
$T^\circ\text{C}$	287	258	240	163	140	140

Table 3. Measurements for the test 2

Test 2	P_1	P_2	P_3	P_4	P_5	P_6
$T^{\circ}\text{C}$	544	528	511	320	320	320

Table 4. Results of computations for the test 1

Test 1	P_1	P_2	P_3	P_4	P_5	P_6
ε						
0.25	289	268	249	149	139	129
0.5	277	256	237	158	146	136
0.75	266	244	228	166	153	142

Table 5. Results of computations for the test 2

Test 1	P_1	P_2	P_3	P_4	P_5	P_6
ε						
0.25	572	551	531	289	279	269
0.5	543	525	511	319	309	300
0.75	525	509	486	352	339	320

$r = R_2, z = 0.1 \text{ m}, 0.5 \text{ m}, 0.9 \text{ m}$ and

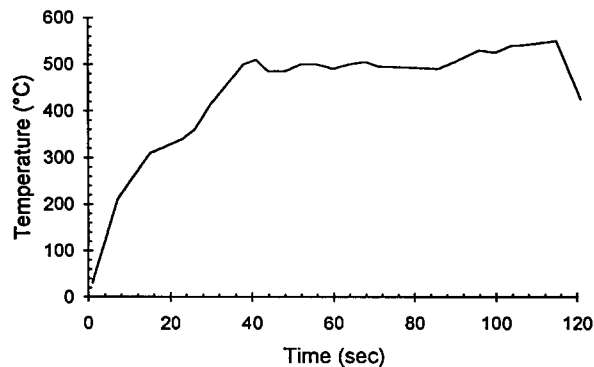
$r = R_4, z = 0.1 \text{ m}, 0.5 \text{ m}, 0.9 \text{ m}$.

The results of the measurements are presented in the Tables 2 and 3.

Our computations have shown that the emissivity ε in (5) is one of the most important parameters of the whole model. This parameter can change from $\varepsilon = 0.25$ (polished steel) over $\varepsilon = 0.5$ (sheet steel) to $\varepsilon = 0.75$ (oxidized steel). Tables 4 and 5 show the results of the computations. It is easy to see that the computational results obtained for $\varepsilon = 0.5$ are very close to the measurements and there is no need to use other parameters to verify the model.

4.2. Geometrical optimization

The aim of our numerical tests on more realistic data presented by Figs. 4 and 5 is to study the influence of the thickness of the inner pipe and of the insulating split on the output temperature $T_{\text{gas}}(t, S)$. The pressure of the exhaust gas is assumed to be constant $p_{\text{gas}} = 1.05 \text{ bar}$.

Fig. 4. Input temperature $T(t, 0)$.

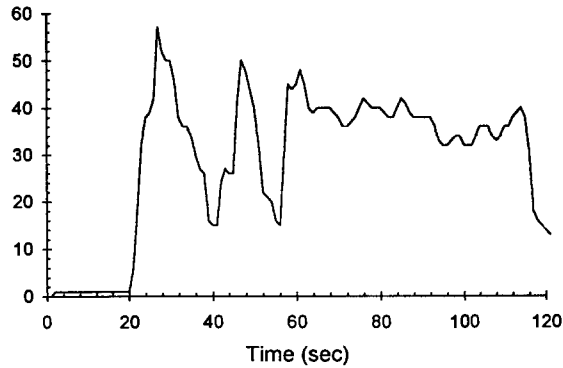


Fig. 5. Input rate of the exhaust gas $m_{\text{gas}}(t)$.

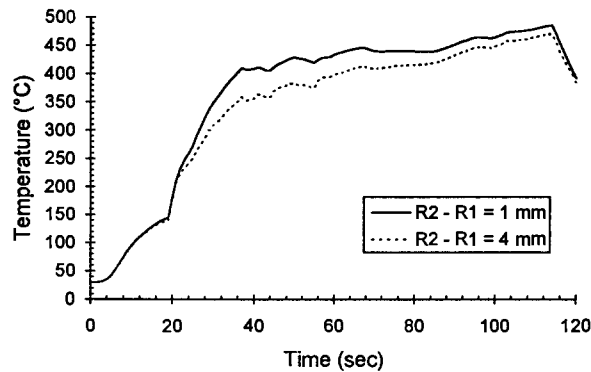


Fig. 6. Output temperature $T_{\text{gas}}(t, S)$ for variable thickness of the inner pipe.

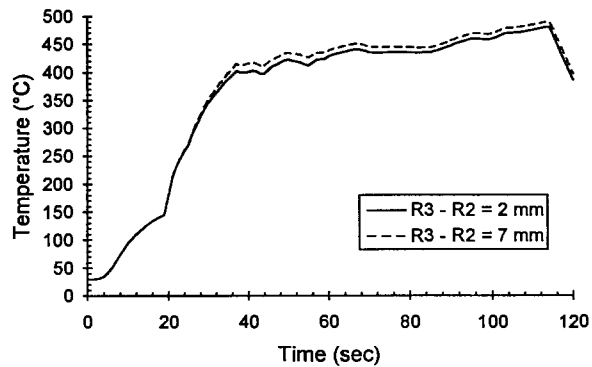


Fig. 7. Output temperature $T_{\text{gas}}(t, S)$ for variable thickness of the insulating split.

The results of our computations are shown in the Figs. 6 and 7. Figure 6 shows the output temperature $T_{\text{gas}}(t, S)$ for variable thickness of the inner pipe with constant thickness (3.5 mm) of the insulating split. Figure 7 shows the output temperature $T_{\text{gas}}(t, S)$ for variable thickness of the insulating split.

Conclusions

1. The insulated exhaust pipe is much more efficient than the usual one, but also more complicated to produce and hence more expensive.
2. From the numerical experiments it is seen that the best way to increase the output temperature $T_{\text{gas}}(t, S)$ is to reduce the heat capacity of the inner pipe.
3. The thickness of the insulating split is not very important for the output temperature and can be chosen from other technical considerations. This result is obtained due to the consideration of the radiation heat transfer.
4. The presented mathematical model and numerical algorithm can be used now, as a first part of complete mathematical model including the exhaust pipe and the catalytic converter itself.
5. The presented algorithm needs only few minutes of CPU time on IBM RISC/6000 for 120 time steps, with the following discretization parameters: $N_1 = 200$, $N_2 = 40 \div 95$ and $\tau = 1$ s.

Acknowledgements

The work was done in the Center for Industrial Mathematics, University of Kaiserslautern. The author is grateful to the 'H. Gillet GmbH', Edenkoben, Germany for financial support and measurements. The author wishes to thank Dr. F.-J. Pfreundt, University of Kaiserslautern, Messrs Krause, H. Bressler and F. Terres from 'H. Gillet GmbH' for many useful discussions during the investigations.

References

1. J. Vardi, and W.F. Biller, Thermal behaviour of an exhaust gas catalytic converter. *I&EC Proc. Dsgn. Dev.* (1968) 83.
2. K. Zygourakis, Transient operation of monolith catalytic converters: A two-dimensional reactor model and the effects of radially nonuniform flow distributions. *Chem. Engng Sci.* 44(9) (1989) 2075–2086.
3. H.-J. Becker, Experimentelle und theoretische Untersuchungen über die instationäre Warmlaufphase unbeschichteter und beschichteter katalysatorwaben, *Dissertation*, Universität Kaiserslautern, 1992.
4. M. Becker, Heat Transfer. A Modern Approach. New York and London, (1986) Plenum Press.
5. R. Siegel and J.R. Howell, *Thermal Radiation Heat Transfer*. Hemisphere Publishing Corp. New York, 1981.
6. A.F. Emery, O. Johansson, M. Lobo and A. Abrons, A comparative study of methods for computing of diffuse radiation viewfactors for complex structures. *J. Heat Transfer*. 113 (1991) 413.
7. M.R. Hestens and E. Stiefel, Methods of conjugate gradients for solving linear systems. *J. Res. NBS* 49 (1952).
8. I. Gustafsson, On modified incomplete factorization methods. *Lect. Notes Math.* 986, (1982) 334–351.
9. A. Friedman (ed.), IMA volumes in mathematics and its application. *Mathematics in Industrial Problems*. Vol. 38, Part 4, Chapter 7, Springer-Verlag, New York.
10. T. Nording, Neuartiges Konzept für isolierte Abgaskrümmen, Vorrohre und Katalysatoren. *Motortechnische Zeitschrift* 52 (1991) 206–210.
11. L.C. Thomas, *Fundamentals of Heat Transfer*. Prentice-Hall Inc. (1980).
12. P.J. Davis, *Circulant Matrices*, John Wiley & Sons, New York (1979).
13. H. May and W. Müller, Spezifische Wärmen, absolute Enthalpien, freie Enthalpien und Entropien verschiedener Stoffe für Temperaturen bis 6000 K. Universität Kaiserslautern (1983).
14. R.J. Le Vegue, *Numerical Methods for Conservation Laws*. Birkhäuser Verlag, Basel-Boston-Berlin (1990).